JOURNAL OF CATALYSIS **176,** 474–487 (1998)
ARTICLE NO. CA982054

Dispersion of Inorganic Salts into Zeolites and Their Pore Modification

Feng-Shou Xiao,[1] Shan Zheng, Jianmin Sun, Ranbo Yu, Shilun Qiu, and Ruren Xu

Department of Chemistry and Key Laboratory of Inorganic Synthesis and Preparative Chemistry, Jilin University, Changchun 130023, People's Republic of China

Received August 19, 1997; revised February 3, 1998; accepted February 23, 1998

A series of samples, prepared from mechanical mixtures of inorganic salts (MoO_3, $CuCl_2$, $NiCl_26H_2O$, and $Ni(NO_3)_26H_2O$) with zeolites (NaZSM-5, NaY, NaY, and MCM-41), have been investigated by X-ray diffraction (XRD), differential thermal analysis (DTA), the adsorption of probing molecules, and the determination of pore size distribution. After the heating of MoO_3 with zeolites at 723 K for 24 h, the samples (MoO_3/NaZSM-5/NaY/MCM-41 = 0–0.088/0–0.24/0–0.45 g/g) show only those X-ray peaks assigned to zeolites, the characteristic peaks of MoO_3 having disappeared completely, which suggests that MoO_3 is highly dispersed in the pores of zeolites. Similar phenomena are observed for the samples of $CuCl_2$/NaZSM-5, $CuCl_2$/NaY, $NiCl_2$/NaZSM-5, $NiCl_26H_2O$/NaY, and $Ni(NO_3)_26H_2O$/NaY. In contrast, the inorganic salts of $NiCl_26H_2O$ and $Ni(NO_3)_26H_2O$ cannot be dispersed into the channels of NaZSM-5 zeolite due to the limitation of the channel size. These results suggest that the dispersion only occurs under the condition that the diameter of the inorganic salts is less or similar to the pore size of the zeolites. Also, we observed that the dispersion capacity of the inorganic salts is strongly related to the pore size of the zeolites. Furthermore, the isotherms for probing molecules show that the dispersion of inorganic salts into zeolites leads to significant change in the pore size of zeolites. The MoO_3/NaY samples exhibit that the pore size was selectively formed at 6.8–8.0, 6.0–6.8, 4.3–6.0, and 3.0–4.3 Å with MoO_3 loading at 0.08, 0.16, 0.21, and 0.24 g/g, respectively. Therefore, it is proposed that we could modify the pore sizes of zeolites to various degrees, which may be very useful to design suitable pores of zeolites for the catalysts in catalytic reactions. Catalytic data in selective reduction of NO by propylene at the temperature of 300°C show that $CuCl_2$/HZSM-5 catalyst prepared from the dispersion method exhibits much higher catalytic conversion (39%: N_2 yield) than that (21%: N_2 yield) of CuZSM-5 catalyst prepared from the ion-exchange method.

Key Words: **dispersion; inorganic salt; pore modification of zeolites; catalytic reduction of NO by hydrocarbons.**

INTRODUCTION

The assembly of active components onto the surface of a support is of importance to chemistry, chemical engineering, and material science. One example of assembling an active phase onto the surface of a support is a supported catalyst, which is usually prepared by metal salts and a support with a high specific surface. Generally, the support includes inorganic oxides (e.g., Al_2O_3 and SiO_2) and zeolites, and the precursors of these active components in catalysts are mostly inorganic salts (1–4). The degree of dispersion of the active component on the support has economic consequences and influences the activity and selectivity of catalysts (1–4), in particular, the active components assembled into zeolites, exhibiting unique catalytic activity and selectivity (5–13). CuZSM-5 catalyst is very active for catalytic decomposition of nitrogen monoxide, and the activity and selectivity are strongly influenced by the copper loading in zeolites (5–9). The novel metal cluster (Rh_6, Ir_6, etc.) entrapped in NaY zeolite is very active for the catalytic hydrogenation and dehydrogenation reactions (10, 11). The Mo-HZSM-5 catalyst exhibits high catalytic selectivity for the conversion from methane to benzene (12, 13). The active components assembled into zeolites offer the advantages both for catalytic active components and for the zeolites.

The methods for preparing the supported catalysts are usually by impregnation (1, 2), ion-exchange (14), and spontaneous monolayer dispersion (15–17). The impregnation method is widely applied to the preparation of various catalysts, and the ion-exchange technique is used for the supports having ion-exchange ability. As compared with impregnation and ion-exchange, the spontaneous monolayer dispersion, as reported by Xie and Tang (15, 17), is relatively simple. They systematically study a series of inorganic salts dispersed on amorphous materials such as γ-Al_2O_3, SiO_2, active carbon, and TiO_2, and find that the dispersion capacity of the inorganic salts is strongly influenced by the surface area of the amorphous materials at the dispersed temperature. The inorganic salts such as MoO_3 disperse spontaneously onto the surface of a support, such as γ-Al_2O_3, and form a close-packed model. Notably, supports such as γ-Al_2O_3 and SiO_2 have a wide distribution of pores in the range of 30–200 Å, but it is not known whether the dispersion of inorganic salts onto the support become size-dependent as the pore size of the zeolites becomes less than 10 Å similar to the kinetic diameter of the inorganic salts.

[1] To whom correspondence should be addressed.

0021-9517/98 $25.00

The research relating to the dispersion of inorganic salts into zeolites are still largely unexplored.

Here, we report (i) the dispersion of the inorganic salts with different kinetic diameters into zeolites, investigating the effect for structures of inorganic salts and for zeolite pores, (ii) the change in pore size of the zeolites by dispersing inorganic salts with various loadings, (iii) the catalytic activity of copper salts highly dispersed into zeolites in selective catalytic reduction of NO by propylene.

EXPERIMENTAL

Materials and Sample Preparation

Inorganic salts such as MoO_3, $CuCl_2 2H_2O$, $NiCl_2 6H_2O$, $Ni(NO_3)_2 6H_2O$, with purity >99.999% (GR), were supplied by Beijing Hongxing Chemical Co. The n-hexane, cyclohexane, and cumene were purified by outgassing and vacuum distillation from a dry ice–methanol cold trap to a liquid nitrogen cold trap. The zeolites such as NaZSM-5 (Si/Al = 40, surface area of about 380 m^2/g), NaY (Si/Al = 2.75, surface area of 750 m^2/g), MCM-41 (Si/Al = 4.5, surface area of 1000 m^2/g) were prepared in our laboratory by using hydrothermal synthesis (14, 18, 19). The γ-Al_2O_3 support (surface area of about 200 m^2/g) was purchased from Merck Co.

The samples were prepared from the mechanical mixtures of inorganic salts with zeolites, followed by heating at the dispersed temperatures. After the preparation, the sample was characterized by X-ray diffraction. The parameters (14, 18, 20, 21) for these samples were listed in Tables 1–2.

Methods of Characterization

The powder X-ray diffraction data were collected on a Rigaku D/Max IIIA diffractometer using CuKα radiation, 40 KV, 30 mA with scanning rate of 4°/min (2θ). The surface area of the supports were measured with nitrogen adsorption methods (BET) by using a Cahn-2000 microbalance at 77 K, and the isotherms such as water, normal-hexane, cyclohexane, and cumene on the samples were carried out with the Cahn-2000 microbalance at room temperature (298 K). The sensitivity of the microbalance was ± 0.1 μg. The pore size distribution for MCM-41 was carried out on the Micrometritics ASAP 2400 automatic adsorption instrument. The distribution of Mo atoms was measured with a Shimadzu EMS-SM-7 electron probe microanalyzer (EPMA) with beam diameter of 2 μm.

TABLE 1

Parameters of Supports (14, 18)

Support	Surface area (m^2/g)	Pore size of zeolite (Å)
NaZSM-5	380	5.6
NaY	750	7.8
MCM-41	1000	Near 30
Al_2O_3	200	30–200

TABLE 2

Parameters of Inorganic Salts (20, 21)

Inorganic salt	Structure of inorganic salt	Dynamic diameter (Å)
MoO_3	Triangle	5.0
$CuCl_2 2H_2O$	Linear	3.6
$NiCl_2 6H_2O$	Octahedral	8–9
$Ni(NO_3)_2 6H_2O$	Octahedral	9–10

Selective Catalytic Reduction of NO by Propylene

Catalytic measurements were carried out in fixed-bed flow reactor operated at atmospheric pressure and temperature at 300°C. Prior to each experiment the catalyst was heated at 320°C in Ar for 2 h, and then cooled to the desired temperature in Ar. A typical reaction mixture contained 1600 ppm NO, 1370 ppm propylene, 2.0% oxygen, with the balance Ar. A 0.5-g sample of the catalyst was used with a total rate of 100 ml/min, and the conversion of NO was based on the amount of N_2 formed. The gas products were analyzed by gas chromatography using Porapak Q (N_2O, CO_2, and hydrocarbons) and molecular sieve 5A (O_2, N_2, NO, CH_4, and CO) columns.

RESULTS

X-Ray Diffraction

MoO_3 on supports. *MoO_3 on γ-Al_2O_3.* The dispersion of MoO_3 on γ-Al_2O_3 has been widely investigated by Xie *et al.* (15, 17). When 0.20 g of MoO_3 is mechanically mixed with 1 g of γ-Al_2O_3 at room temperature, the XRD patterns give characteristic of MoO_3 and γ-Al_2O_3. However, when the sample is heated for 24 h at 773 K, the XRD peaks assigned to MoO_3 in the sample completely disappear. The phenomenon suggests high dispersion of MoO_3 on the surface of the γ-Al_2O_3 support, where MoO_3 no longer exists in crystalline state. Notably, when the content of MoO_3 in the mixture with the γ-Al_2O_3 support exceeded a critical amount, the peaks of crystalline MoO_3 appear, but were markedly reduced after the heat treatment. The critical dispersion capacity of MoO_3 on the surface of the Al_2O_3 support is 0.24 g/g (15, 17).

MoO_3 on NaZSM-5. A series of MoO_3/NaZSM-5 samples were prepared by the mechanical mixtures of NaZSM-5 zeolite with various MoO_3 loadings (weight ratio of MoO_3 to NaZSM-5 at 0.026, 0.053, 0.07, 0.088, 0.105, 0.158, 0.210 g/g), followed by heating at 723 K for 24 h.

Figure 1 shows the XRD patterns of MoO_3/NaZSM-5 samples before and after heating treatment. As observed in Fig. 1b, the XRD peaks give rise to the characteristic of

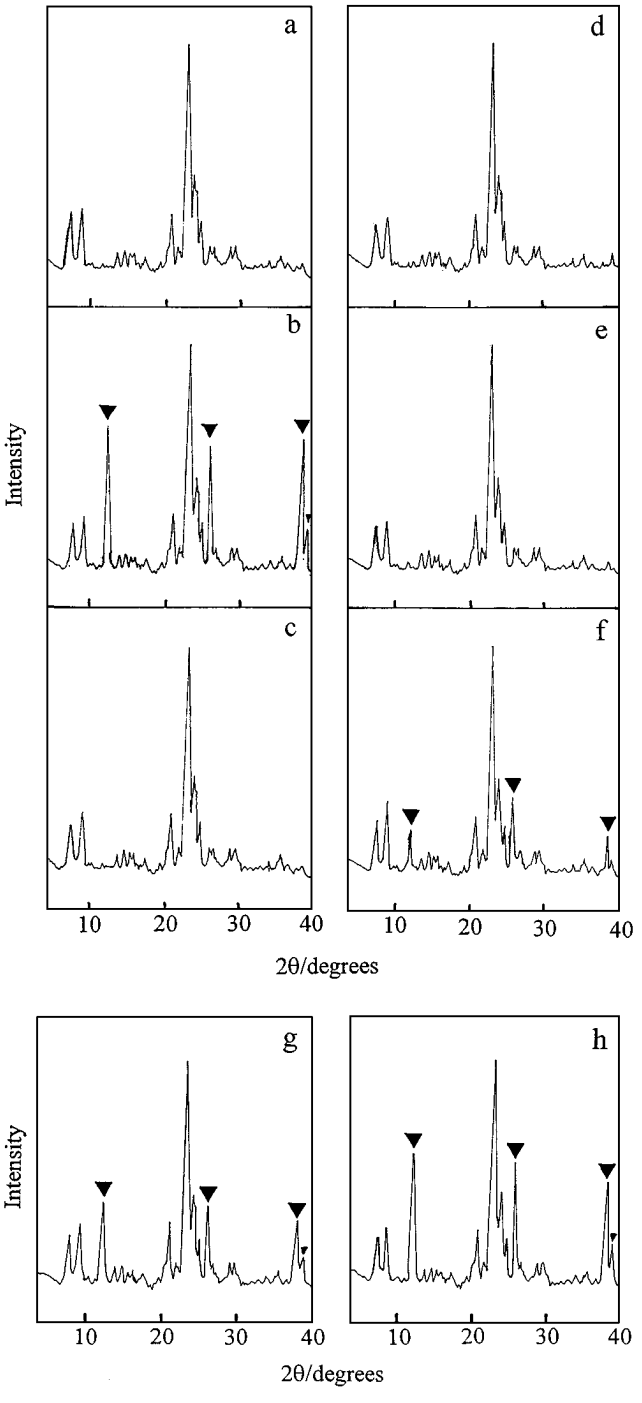

FIG. 1. XRD patterns of NaZSM-5 zeolite with various MoO_3 loading: (a) NaZSM-5 zeolite; (b) mechanical mixture of 0.026 g of MoO_3 and 1.0 g of NaZSM-5 zeolite; (c) mechanical mixture of 0.026 g of MoO_3 and 1.0 g of NaZSM-5 zeolite, followed by heating at 723 K for 24 h; (d) mechanical mixture of 0.053 g of MoO_3 and 1.0 g of NaZSM-5 zeolite, followed by heating at 723 K for 24 h; (e) mechanical mixture of 0.088 g of MoO_3 and 1.0 g of NaZSM-5 zeolite, followed by heating at 723 K for 24 h; (f) mechanical mixture of 0.105 g of MoO_3 and 1.0 g of NaZSM-5 zeolite, followed by heating at 723 K for 24 h; (g) mechanical mixture of 0.158 g of MoO_3 and 1.0 g of NaZSM-5 Zeolite, followed by heating at 723 K for 24 h; (h) mechanical mixture of 0.210 g of MoO_3 and 1.0 g of NaZSM-5 zeolite, followed by heating at 723 K for 24 h (▼: XRD peaks of MoO_3).

crystalline MoO_3 and NaZSM-5 structure. It is of interest to note that the characteristic peaks assigned to crystalline MoO_3 disappear completely when the sample is heated for 24 h at 773 K, as given in Fig. 1c. The disappearance of the XRD peaks of MoO_3 crystal in the sample might be also explained by high dispersion of MoO_3 into the channel of the NaZSM-5 zeolite, where the MoO_3 no longer exists in the crystalline state (15, 22–24). Increasing the MoO_3 loading in NaZSM-5 zeolite up to 0.088 g/g, we still could not observe the XRD peaks of MoO_3 crystalline, as shown in Figs. 1c–1e. Upon further increase of MoO_3 loading in NaZSM-5 zeolite over 0.088 g/g, the characteristic peaks assigned to MoO_3 crystalline appear, indicating the presence of crystalline MoO_3 in the samples, as given in Figs. 1f–1h.

The amount of residual crystalline MoO_3 can be determined by XRD quantitative phase analysis (25). Here, we use an inner standard, namely α-Al_2O_3, added to MoO_3/NaZSM-5 samples and measure the peak area for reflections 110 and 021 of MoO_3 and 113 of α-Al_2O_3. The peak intensity ratio $I_{MoO_3}/I_{\alpha\text{-}Al_2O_3}$ is reasonably assumed to be proportional to the ratio of the content of crystalline MoO_3 to that of α-Al_2O_3, as

$$I_{MoO_3}/I_{\alpha\text{-}Al_2O_3} = k \times M_{MoO_3}/M_{\alpha\text{-}Al_2O_3},$$

where I and M stand for XRD intensity and weight percentage, respectively, and k is a proportionality constant determined from a sample of known phase composition. With known content of α-Al_2O_3, the weight percentage of crystalline MoO_3 can be derived from the intensity ratio of $I_{MoO_3}/I_{\alpha\text{-}Al_2O_3}$. For a series of MoO_3/NaZSM-5 samples, we have obtained plots of the residual amount of crystalline MoO_3 versus the total amount of MoO_3 into NaZSM-5 zeolites, as shown Fig. 2. From the plots one can find a threshold at 0.088 g MoO_3/g NaZSM-5, corresponding the critical dispersion capacity. When the content of MoO_3 in the sample is below this threshold value, no crystalline MoO_3 can be detected. If the MoO_3 content exceeds this threshold, the

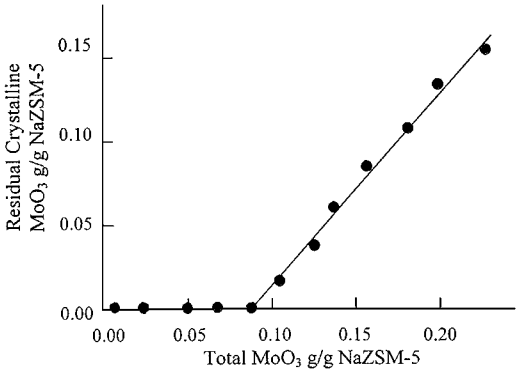

FIG. 2. Residual amount of MoO_3 versus total amount of MoO_3 in MoO_3/NaZSM-5 samples prepared by dispersion of MoO_3 into NaZSM-5 zeolite at 723 K for 24 h.

residual amount of MoO_3 increases with the total amount of MoO_3, as is shown by the straight line in the plots. Similarly, the dispersion capacity of each salt into the zeolite is found by the same method.

MoO_3 on NaY. A series of MoO_3/NaY samples were prepared by the mechanical mixtures of NaY zeolite with various MoO_3 loadings (weight ratio of MoO_3 to NaY in 0–0.40 g/g), followed by heating at 673 K for 24 h. The results demonstrate that MoO_3 is highly dispersed in the pores of NaY zeolite with MoO_3 loadings of 0–0.240 g/g. Obviously, the dispersion capacity of MoO_3 on NaY zeolite is much higher (almost 3 times) than that on NaZSM-5 zeolite.

MoO_3 on NaA. A series of MoO_3/NaA samples were prepared by the mechanical mixtures of NaA zeolite with various MoO_3 loadings (weight ratio of MoO_3 to NaA in 0–0.20 g/g), followed by heating at 673 K for 24 h. The XRD patterns of these samples show characteristic peaks of MoO_3 crystalline and NaA zeolite, indicating that MoO_3 could not disperse into NaA zeolite.

MoO_3 on MCM-41. The MoO_3/MCM-41 samples were prepared by the mechanical mixtures of MCM-41 molecular sieve with various MoO_3 loadings (weight ratio of MoO_3 to MCM-41 in 0–0.60 g/g), followed by heating at 673 K for 24 h. We observed that the dispersion capacity on MCM-41 molecular sieve is very high, as compared with those on NaZSM-5 and NaY zeolites. Even the weight ratio of MoO_3 to MCM-41 at 0.45 g/g, we still could not observe characteristic XRD peaks of MoO_3 crystalline. With a further increase in MoO_3 loading in MCM-41 molecular sieve to 0.50 g/g, the crystallinity (2θ at 1–4°) assigned to MCM-41 molecular sieve slightly decreases, which may be related to the change in the structure of MCM-41 molecular sieve.

$CuCl_2$ on supports. $CuCl_2$ on Al_2O_3. The dispersion capacity of $CuCl_2$ on γ-Al_2O_3 is 0.20 g/g, suggested by "*submonolayer dispersion*" (15).

$CuCl_2$ on NaZSM-5. A series of $CuCl_2$/NaZSM-5 samples were prepared by the mechanical mixtures of NaZSM-5 zeolite with various $CuCl_2$ loadings (weight ratio of $CuCl_2 2H_2O$ to NaZSM-5 in 0.111–0.443 g/g), followed by heating at 673 K for 24 h, as shown in Fig. 3. The results indicate that the dispersion capacity of $CuCl_2 2H_2O$ into NaZSM-5 zeolite is about 0.22 g/g. In general, the dehydration of $CuCl_2 2H_2O$ occurred at near 393 K. Therefore, under heating at 673 K the $CuCl_2 2H_2O$ is dehydrated to $CuCl_2$. However, after exposure to air for 6 h at room temperature, the $CuCl_2$ into NaZSM-5 zeolite hydrated again, forming $CuCl_2 2H_2O$ in the sample.

$CuCl_2$ on NaY. A series of $CuCl_2$/NaY samples were prepared by the mechanical mixtures of NaY zeolite with various $CuCl_2$ loadings (weight ratio of $CuCl_2 2H_2O$ to NaY at 0.222, 0.443, 0.665, and 0.883 g/g), followed by heating at 723 K for 24 h. The results indicate that the dispersion capacity of $CuCl_2 2H_2O$ on NaY zeolite is about 0.44 g/g.

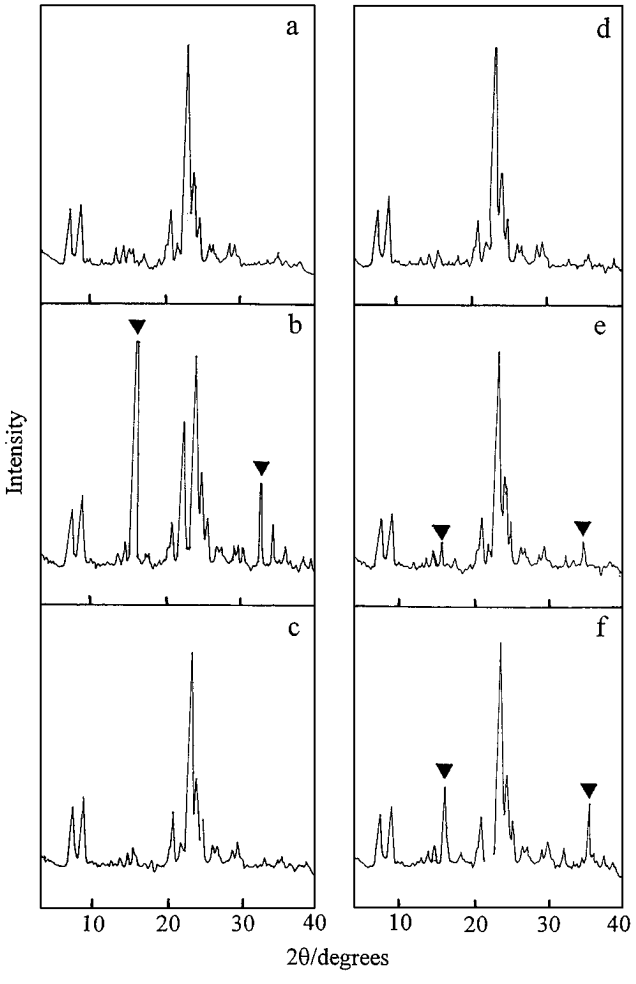

FIG. 3. XRD patterns of NaZSM-5 zeolite with various $CuCl_2$ loading: (a) NaZSM-5 zeolite; (b) mechanical mixture of 0.111 g of $CuCl_2 2H_2O$ and 1.0 g of NaZSM-5 zeolite; (c) after b, followed by heating at 673 K for 24 h; (d) mechanical mixture of 0.222 g of $CuCl_2 H_2O$ and 1.0 g of NaZSM-5 zeolite, followed by heating at 673 K for 24 h; (e) mechanical mixture of 0.333 g of $CuCl_2 2H_2O$ and 1.0 g of NaZSM-5 zeolite, followed by heating at 673 K for 24 h; (f) mechanical mixture of 0.443 g of $CuCl_2 2H_2O$ and 1.0 g of NaZSM-5 zeolite, followed by heating at 673 K for 24 h (▼: XRD peaks of $CuCl_2 2H_2O$).

$NiCl_2 6H_2O$ on supports. $NiCl_2 6H_2O$ on γ-Al_2O_3. The dispersion capacity of $NiCl_2$ on γ-Al_2O_3 is 0.17 g/g, suggested by "*monolayer dispersion*" (15). As compared with the other inorganic salts, the dispersed temperature of nickel salts is relatively low; e.g., high dispersion of $NiCl_2 6H_2O$ on the surface of γ-Al_2O_3 proceeds at room temperature.

$NiCl_2 6H_2O$ on NaZSM-5. A series of $NiCl_2$/NaZSM-5 samples were prepared by the mechanical mixtures of NaZSM-5 zeolite with various $NiCl_2$ loadings (weight ratio of $NiCl_2 6H_2O$ to NaZSM-5 at 0.076, 0.157, and 0.305 g/g), and their XRD patterns are shown in Fig. 4. As observed in Figs. 4b–4e, the XRD peaks of mechanical mixtures with mass ratio of $NiCl_2 6H_2O$/NaZSM-5 at 0.305 and 0.157 g/g,

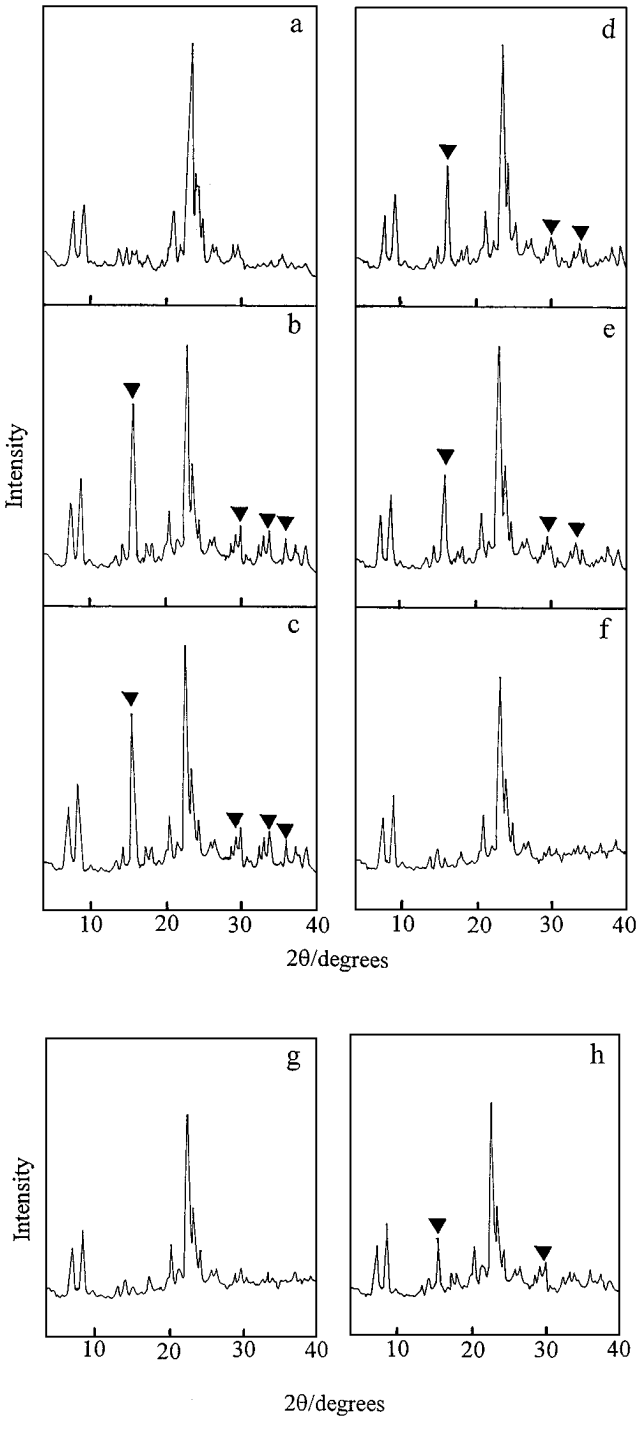

FIG. 4. XRD patterns of NaZSM-5 zeolite with various $NiCl_2$ loadings: (a) NaZSM-5 zeolite; (b) mechanical mixture of 0.305 g of $NiCl_26H_2O$ and 1.0 g of NaZSM-5 zeolite; (c) after b, followed by placement at room temperature for 36 h; (d) mechanical mixture of 0.157 g of $NiCl_26H_2O$ and 1.0 g of NaZSM-5 zeolite; (e) after d, followed by placement at room temperature for 36 h; (f) mechanical mixture of 0.076 g of $NiCl_26H_2O$ and 1.0 g of NaZSM-5 zeolite, followed by heating at 433 K for 36 h; (g) mechanical mixture of 0.157 g of $NiCl_26H_2O$ and 1.0 g of NaZSM-5 zeolite, followed by placement at 433 K for 36 h; (h) mechanical mixture of 0.305 g of $NiCl_26H_2O$ and 1.0 g of NaZSM-5 zeolite, followed by treatment at 443 K for 36 h (▼: XRD peaks of $NiCl_26H_2O$).

are the same as those of the samples treated at room temperature for 36 h, indicating that the dispersion of $NiCl_26H_2O$ into the channel of NaZSM-5 zeolite does not occur.

It is of interest to note that the XRD peaks assigned to $NiCl_26H_2O$ crystalline in the mechanical mixtures with $NiCl_26H_2O$/NaZSM-5 at 0.157 and 0.305 g/g completely disappear after the mixtures are heated at 433 K for 24 h, as shown in Figs. 4f and 4g. These results indicate that heating at 433 K for $NiCl_26H_2O$/NaZSM-5 mixtures leads to the high dispersion of $NiCl_2$ into NaZSM-5 zeolite. A further increase of $NiCl_26H_2O$ loading in NaZSM-5 zeolite, the characteristic peaks assigned to $NiCl_26H_2O$ crystalline appear again, suggesting the dispersion capacity of $NiCl_26H_2O$ in NaZSM-5 at about 0.305 g/g.

$NiCl_26H_2O$ on NaY. A series of $NiCl_26H_2O$/NaY samples were prepared by the mechanical mixtures of NaY zeolite with various $NiCl_2$ loadings (weight ratio of $NiCl_26H_2O$ to NaY at 0.152, 0.305, 0.609, and 0.914 g/g), followed by placement at room temperature for 36 h. As different with those in $NiCl_26H_2O$/NaZSM-5 samples, the placement at room temperature for $NiCl_26H_2O$/NaY mixtures results in disappearance of characteristic peaks of $NiCl_26H_2O$ crystalline, which suggests that the high dispersion of $NiCl_26H_2O$ into the pores of NaY zeolites occurs at room temperature.

$Ni(NO_3)_26H_2O$ on supports. $Ni(NO_3)_26H_2O$ on NaZSM-5. A series of $Ni(NO_3)_26H_2O$/NaZSM-5 samples were prepared by the mechanical mixtures of NaZSM-5 zeolite with various $Ni(NO_3)_2$ loadings (weight ratio of $Ni(NO_3)_26H_2O$ to NaZSM-5 at 0.20 and 0.30 g/g), followed by placement at room temperature for 36 h. We observed that the characteristic XRD patterns of $Ni(NO_3)_26H_2O$/NaZSM-5 are the same before and after the treatment. The results indicate that the $Ni(NO_3)_26H_2O$ could not disperse into the channels of NaZSM-5 zeolite at room temperature.

$Ni(NO_3)_26H_2O$ on NaY. A series of $Ni(NO_3)_26H_2O$/NaY samples were prepared by the mechanical mixtures of NaY zeolite with various $Ni(NO_3)_2$ loadings (weight ratio of $Ni(NO_3)_26H_2O$ to NaY at 0.13 and 0.16 g/g), followed by placement at room temperature for 36 h. XRD results showed that characteristic of peaks assigned to $Ni(NO_3)_26H_2O$ disappear completely after placement of $Ni(NO_3)_26H_2O$/NaY at room temperature for 36 h, which indicates that the $Ni(NO_3)_26H_2O$ could disperse into the pores of NaY zeolites at room temperature.

Thermal Analysis

Figure 5 shows the curves of DTA for various samples of $CuCl_22H_2O$/NaZSM-5. NaZSM-5 sample shows one peak at 360 K in DTA curve (Fig. 5a), which is assigned to the desorption of water adsorbed on NaZSM-5. The DTA curve of $CuCl_22H_2O$ shows two peaks at 400 and 773 K (Fig. 5b), which are attributed to the dehydration of $CuCl_22H_2O$ and the melting point of $CuCl_2$, respectively.

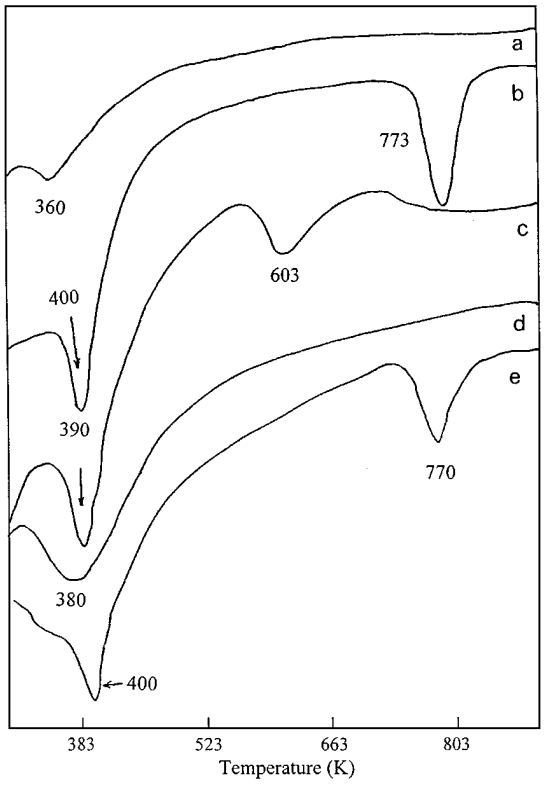

FIG. 5. DTA curves of (a) NaZSM-5, (b) $CuCl_2 2H_2O$, (c) mechanical mixture of $CuCl_2 2H_2O$ and NaZSM-5 with weight ratio of $CuCl_2 2H_2O$/NaZSM-5 of 0.1 g/g, (d) mechanical mixture of $CuCl_2 2H_2O$ and NaZSM-5 with weight ratio of $CuCl_2 2H_2O$/NaZSM-5 of 0.1 g/g, followed by heating at 723 K for 24 h, (e) mechanical mixture of $CuCl_2 2H_2O$ and NaZSM-5 with weight ratio of $CuCl_2 2H_2O$/NaZSM-5 of 0.45 g/g, followed by heating at 723 K for 24 h.

The mechanical mixture of $CuCl_2 2H_2O$ with NaZSM-5 (weight ratio, 0.1 g/g) give two strong peaks at 390 and 603 K (Fig. 5c). The peak at 390 K is very similar to the peak at 400 K assigned to the dehydration of $CuCl_2 2H_2O$ in Fig. 5b, and thus we assigned this peak to the dehydration of $CuCl_2 2H_2O$/NaZSM-5. The peak at 603 K is attributed to *high dispersion* of $CuCl_2 2H_2O$ into NaZSM-5 zeolite. Similar phenomena have been studied extensively in the systems of inorganic salts with oxides such as γ-Al_2O_3 (15). Furthermore, after the heating of $CuCl_2 2H_2O$ with NaZSM-5 at 723 K for 24 h, the sample profile exhibits only a peak at 380 K assigned to the dehydration of the sample, the peak at 603 K in Fig. 5c and the peak at 773 in Fig. 5b completely disappears. The results suggest that there is no $CuCl_2 2H_2O$ crystalline phase in the sample, indicating that $CuCl_2 2H_2O$ highly dispersed into NaZSM-5 zeolite. When $CuCl_2 2H_2O$ loading in NaZSM-5 is increased to a weight ratio of 0.45 g/g heated at 723 K for 24 h (threshold value at 0.22 g/g), the sample DTA curve exhibits two peaks at 400 and 770 K. The peak at 400 K is assigned to the dehydration of the sample, and the other peak at 770 K, is assigned to the melting point of $CuCl_2$ crystalline, indicating that residual crystalline phase of $CuCl_2 2H_2O$ exists in $CuCl_2 2H_2O$/NaZSM-5 sample ($CuCl_2 2H_2O$/NaZSM-5 ratio of 0.45 g/g).

In addition, we extended our investigation to MoO_3/NaZSM-5, MoO_3/NaY, and MoO_3/NaA systems heated at 723 K for 24 h, and it is found that in MoO_3/NaZSM-5 and MoO_3/NaY samples (below their threshold value) the peak assigned to melting point of MoO_3 crystalline disappear, and all MoO_3/NaA samples exhibit a strong peak assigned to the melting point of crystalline MoO_3.

Isotherms Measurements

As typical runs, the studies for isotherms measurements were mainly performed on the MoO_3/NaZSM-5 and MoO_3/NaY samples.

MoO_3 on NaZSM-5. In general, the channel of NaZSM-5 has the pore size of 5.6 Å (26) which easily adsorb both normal-hexane and water. However, the dispersion of MoO_3 into NaZSM-5 leads to the change in channel size significantly. Figure 6 shows water and hexane isotherms on the MoO_3/NaZSM-5 sample (MoO_3/NaZSM-5 ratio of 0.088 g/g) treated by heating at 723 K for 24 h. We observed that the water isotherm exhibits typical Langmuir adsorption on the sample with adsorption amount of 6.5 mg/g,

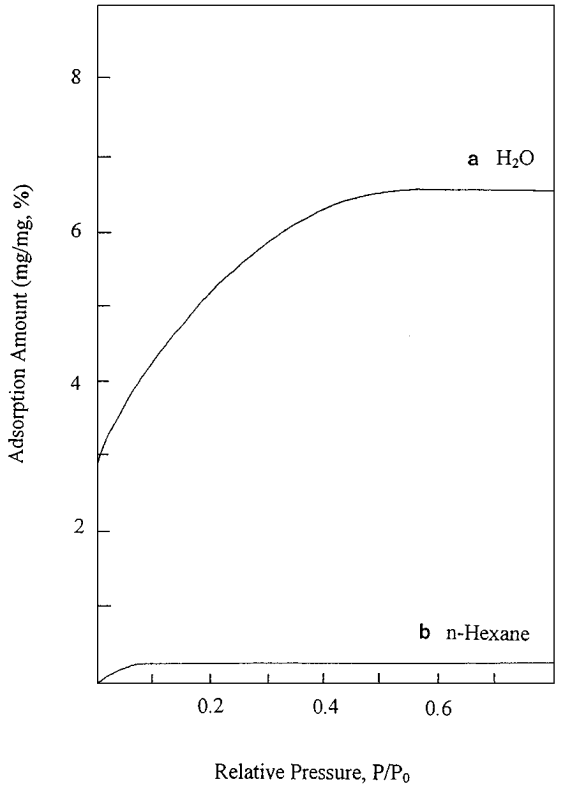

FIG. 6. The isotherms for (a) water and (b) normal hexane on the mixture of 0.088 g of MoO_3 and 1 g of NaZSM-5 zeolite treated by heating at 723 K for 24 h.

suggesting typical of micropore filling (14, 18). However, the water isotherms requires a higher vapor pressure to reach saturated adsorption, as compared with those on NaZSM-5 and the mechanical mixture of MoO_3-NaZSM-5 sample with the same MoO_3 loading (18). The phenomenon may be related to the change in channel shape in the zeolite, which strongly influences the adsorption of water on the sample.

In contrast, we found that the MoO_3/NaZSM-5 sample (MoO_3/NaZSM-5 ratio of 0.088 g/g, heating at 723 K for 24 h) could not adsorb the n-hexane, which indicates that the channels in the MoO_3/NaZSM-5 sample at MoO_3/NaZSM-5 ratio of 0.088 g/g, are less than 4.3 Å (the dynamic diameter of normal hexane at 4.3 Å), which are filled by the MoO_3 component.

MoO_3 on NaY. Figures 7–10 show isotherms for various probing molecules on a series of MoO_3/NaY samples treated by heating at 673 K for 24 h with MoO_3/NaY ratio at 0.08, 0.16, 0.21, and 0.24 g/g, respectively. The MoO_3/NaY sample with MoO_3/NaY ratio at 0.08 g/g shows Langmuir-type adsorption for cumene, cyclohexane, normal-hexane, and water with the critical molecular diameter in the ranged of 6.8–3.0 Å, and Fig. 7 shows the cumene isotherm at room temperature. Increasing the MoO_3 loading in NaY zeolite to 0.16 g/g, the sample shows Langmuir-type adsorption for cyclohexane, but it does not adsorb cumene, as shown in Fig. 8. With an increase of MoO_3 loading in NaY zeolite to 0.21 g/g, the sample exhibits Langmuir-type isotherm for normal-hexane, but the adsorption for cyclohexane is very difficult (less 0.5 mg/g), as shown in Fig. 9. Upon further increase of MoO_3 loading in NaY zeolite to 0.24 g/g, the sample only adsorbs water, as shown in Fig. 10.

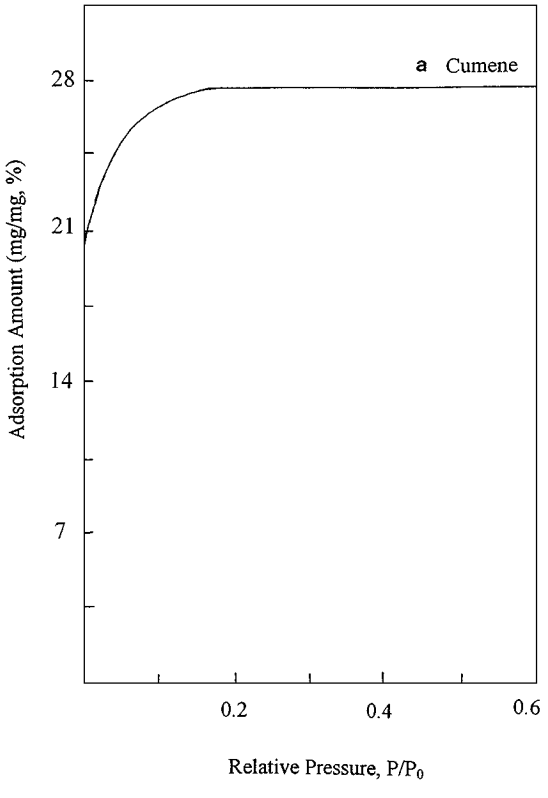

FIG. 7. Cumene isotherm on the mixture of 0.08 g of MoO_3 and 1 g of NaY zeolite treated by heating at 673 K for 24 h.

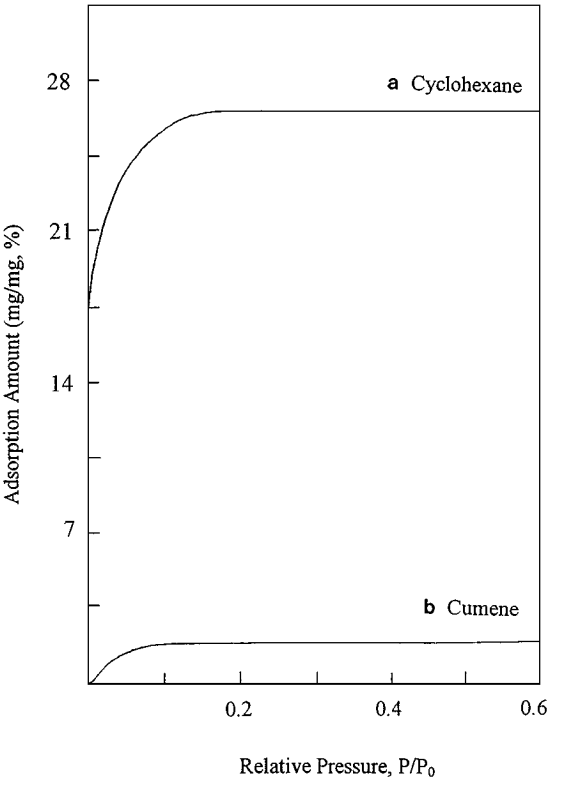

FIG. 8. The isotherms for (a) cyclohexane and (b) cumene on the mixture of 0.16 g of MoO_3 and 1 g of NaY zeolite treated by heating at 673 K for 24 h.

Pore Size Distribution

Figure 11 shows determination of pore size distribution for the MCM-41 molecular sieve and MoO_3/MCM-41 mixture (weight ratio at 0.45 g/g) by nitrogen adsorption at 77 K. In contrast to pore (about 30 Å) of the MCM-41, the pore of MoO_3/MCM-41 mixture reduces obviously (about 25 Å), which is strongly related to the high dispersion of MoO_3 on the pores of MCM-41 molecular sieve.

Electron Probe Microanalyzer

The electron probe microanalyzer (EPMA) was used to investigate the distribution of inorganic salts into zeolites. For example, after dispersion of MoO_3 into NaZSM-5 (MoO_3/NaZSM-5 ratio of 0.05 g/g) by heating at dispersed temperature, the Mo species is determined at the sample crystal paralleled *c* axis, as shown in Fig. 12. The EPMA

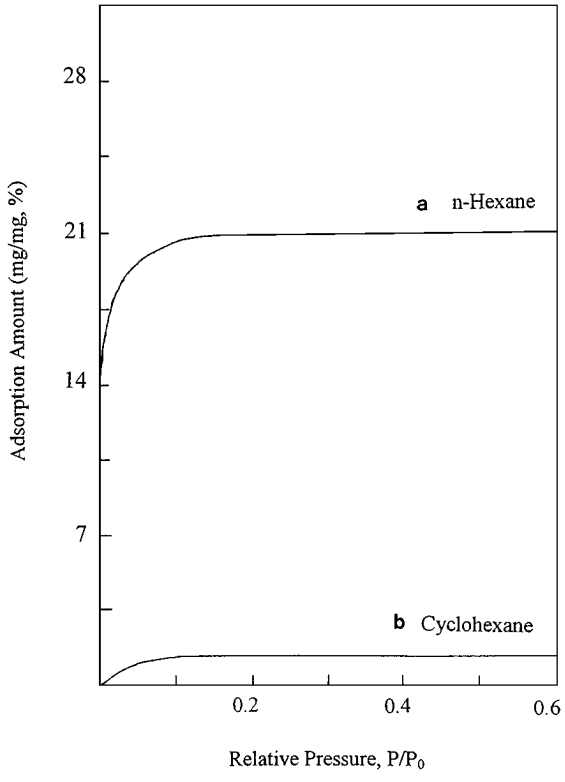

FIG. 9. The isotherms for (a) normal hexane and (b) cyclohexane on the mixture of 0.21 g of MoO_3 and 1 g of NaY zeolite treated by heating at 673 K for 24 h.

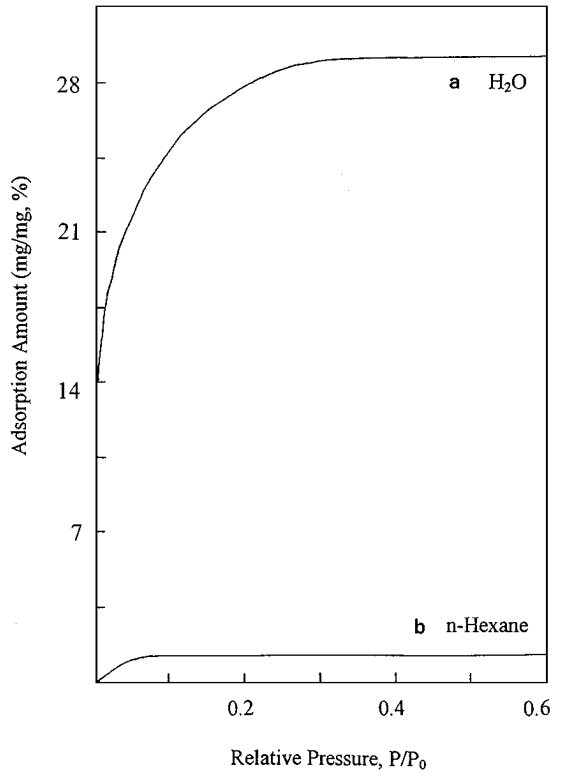

FIG. 10. The isotherms for (a) water and (b) normal hexane on the mixture of 0.24 g of MoO_3 and 1 g of NaY zeolite treated by heating at 673 K for 24 h.

results of four points exhibit the similar value at 0.05 g/g for MoO_3.

Selective Catalytic Reduction of NO by Propylene

An application of the dispersion of inorganic salts into zeolites is to prepare the copper/zeolite catalysts with high copper loading. Table 3 presents catalytic conversion at the temperature of 573 K in selective catalytic reduction of NO by propylene in the presence of excessive oxygen over a series of copper/zeolite samples prepared from dispersion method. The catalytic conversion was measured by N_2 yield. The samples of NaZSM-5, HZSM-5, $CuCl_2$ + NaZSM-5, $CuCl_2$/NaZSM-5 (samples 1–3 and 6) exhibit low conversion as compared with ion-exchanged CuZSM-5 (sample 4). However, the sample prepared from dispersion of $CuCl_2$ into HZSM-5 (sample 5) give much higher conversion. These results suggest that copper species highly dispersed into channels of HZSM-5 zeolite is very effective for improvement of the catalytic activity.

Infrared spectroscopy for ν_{OH} in the region from 3000 to 4000 cm^{-1} shows that the sample of $CuCl_2$/HZSM-5 (sample 5) gives a sharp band at 3610 cm^{-1} assigned to strong acidic OH groups, which is identical with that of HZSM-5 (sample 2) (28–30). Similarly, the sample of CuZSM-5 (sample 4) gives the same band at 3610 cm^{-1} to that of HZSM-5 (28–30). On the contrary, we could not observe the band at 3610 cm^{-1} in the samples of NaZSM-5 and $CuCl_2$/NaZSM-5 (samples 1 and 6).

Accordingly, 100% ion-exchange of Cu^{2+} with NaZSM-5 and HZSM-5 would result in the formation of CuZSM-5 with a full removal of sodiums and protons in ZSM-5 zeolite

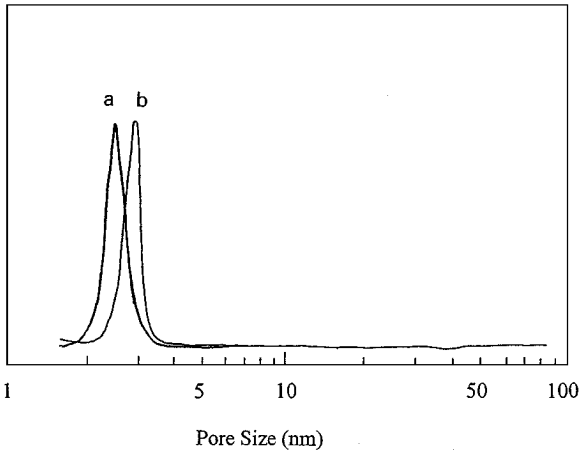

FIG. 11. (a) the pore distribution curve of MCM-41 molecular sieve, and (b) the pore distribution curve of MoO_3/MCM-41 sample (weight ratio at 0.45 g/g, heated at 723 K for 24 h).

TABLE 3

Catalytic Activity in Selective Catalytic Reduction of NO by Propylene over Zeolite-Supported Copper Samples Prepared from Mechanical Mixture, Dispersion, and Ion-Exchange Methods

Sample	Catalyst	Preparation method of catalyst	Copper loading (wt%)	Catalytic conv.[a] (%)	3610 cm^{-1} in IR band[b]
1	NaZSM-5		0	<5	N
2	HZSM-5		0	<10	Y
3	$CuCl_2$ + NaZSM-5	Mechanical	4.8	<5	N
4	CuZSM-5	Ion-exchange	1.8	18	Y
5	$CuCl_2$/HZSM-5	Dispersion	4.8	39	Y
6	$CuCl_2$/NaZSM-5	Dispersion	4.8	<5	N

[a] Catalytic conversion was estimated on N_2 yield at 300°C.
[b] Y represents that the sample showed 3610 cm^{-1} band, and N means that no 3610 cm^{-1} band was observed in IR spectroscopy.

(14, 28). In fact, CuZSM-5 (sample 4) prepared from $CuCl_2$ aqueous solution exhibit the same band at 3610 cm^{-1}, as compared with that of HZSM-5 (sample). Moreover, the most value for ion-exchange of Cu^{2+} with NaZSM-5 and HZSM-5 is approximately 1.0 of Cu^{2+}/Al (14, 28). These results suggested that there might be some reactions in the aqueous solution for ion-exchange. We proposed that the Cu^{2+} ion-exchanged with NaZSM-5 and HZSM-5 to give [Cu(OH)]ZSM-5, showing highest ion-exchanged value at 1.0 of Cu/Al and the strong band at 3610 cm^{-1} assigned to acidic OH groups (28–30).

DISCUSSION

The dispersion of oxides or salts on the surface of supports such as γ-Al_2O_3, are systematically investigated by the pioneers Tang, Xie, and Gui *et al.* (15, 17) and they find the dispersion capacity of salts is mainly related to the surface area; thus they suggest the model such as "monolayer dispersion" or "submonolayer dispersion." Furthermore, they extend these studies to salt/zeolite systems, and it is found that the model on the surface of γ-Al_2O_3 is not in agreement with that on salt/zeolite systems. On the other hand, the dispersion of inorganic salts into zeolites may lead to the change in pore size, adsorption ability, and catalytic properties. A series of systems need to be investigated in detail.

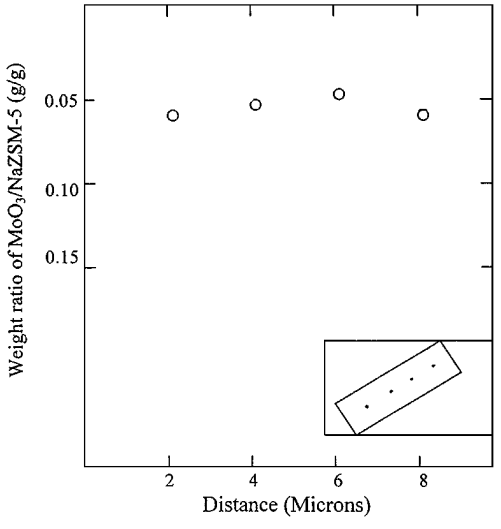

FIG. 12. Distribution of Mo atoms in NaZSM-5 crystal dispersed by MoO_3 at 723 K for 24 h (MoO_3/NaZSM-5 = 0.05). The EPMA results of four points were determined in NaZSM-5 crystal paralleled *c* axis.

The Dispersion of Inorganic Salts onto Surface of Supports

MoO_3 on supports. MoO_3 on γ-Al_2O_3. γ-Al_2O_3 supports have a wide pore distribution in the range of 30–200 Å, and MoO_3 highly disperses on the surface of the γ-Al_2O_3 support as a *close-packed monolayer model* (15, 17). The threshold value of the MoO_3 dispersion amount on the surface of Al_2O_3 is 0.24 g/g of MoO_3/Al_2O_3 ratio, corresponding to dispersion capacity of 0.12 g for 100 m^2 of Al_2O_3 surface. In other words, a "molecule" of MoO_3 occupies 20 $Å^2$, which is in good agreement with the results obtained by Fransen *et al.* (27) from their preparative work by means of adsorption in gas and solution of 17 and 22 $Å^2$/molecule of MoO_3, respectively.

MoO_3 on NaZSM-5. As compared with Al_2O_3 support, the dispersion amount of MoO_3 into the channels of NaZSM-5 is relatively low, corresponding to the dispersion capacity of 0.025 g for 100 m^2 of NaZSM-5 zeolite, which is only 21% for the dispersion of MoO_3 on γ-Al_2O_3 surface (Fig. 1).

The pore distribution of γ-Al_2O_3 support is in the range of 30–200 Å, but the channel of NaZSM-5 zeolite is uniform of 5.6 Å. It is thus suggested that the channel of NaZSM-5 zeolite limits the dispersion of MoO_3. Considering the MoO_3 with C_{3V} point group has a dynamic diameter of 5.0 Å (20, 21), it is reasonable that each MoO_3 could occupy the entire pore (*l*) of NaZSM-5 channel of 5.6 Å. Based on this postulation, the internal surface area occupied by each

MoO_3 should be calculated in the following equation:

$$A = \pi dl = \pi \times 6.0\ \text{Å} \times 5.0\ \text{Å} = 94.2\ \text{Å}^2, \quad [1]$$

where d stands for the diameter of the channel, and l represents for the distance occupied by MoO_3 in the channel, and A stands for the internal surface area occupied by each MoO_3 molecule.

On the other hand, the surface area of NaZSM-5 zeolite is 350 m^2/g, therefore each gram of NaZSM-5 zeolite could disperse a total number of MoO_3 molecules according to

$$N = S/A = 350\ \text{m}^2/94.2\ \text{Å}^2 = 3.7 \times 10^{20}, \quad [2]$$

where N refers as the number of MoO_3 dispersed into zeolite channels, and S is surface area of NaZSM-5 zeolite.

Based on Eqs. [1] and [2], we calculate the theoretical dispersion capacity of MoO_3 into NaZSM-5 zeolite as

$$W = (N/6.023 \times 10^{23})M = (3.7 \times 10^{20}/6.023 \times 10^{23}) \times 144 = 0.888\ (\text{g}), \quad [3]$$

where W represents for theoretical dispersion amount of MoO_3 into NaZSM-5 zeolite, and M is molecular weight of MoO_3.

Notably, the theoretical value is consistent with our experimental results.

The mechanism of salts into pores of zeolites is interpreted by the change in free energy ($\Delta G < 0$). Normally, a process that disperses a substance in a crystalline state as a monolayer or submonolayer into the pores of zeolites would gain in entropy. If this process is energetically not so unfavorable as to reverse its trend, the free enthalpy would be decreased and so occurs the spontaneity. As a formula, this process is given as

$$\Delta G = \Delta H - T\Delta S \quad \text{(first and second laws of thermodynamics)}, \quad [4]$$

where ΔG stands for change in free energy, ΔH is the change in enthalpy, and ΔS is the change in the entropy, respectively.

The dispersion of inorganic salts into zeolites means increasing disorder for the inorganic salts. While the disorder of inorganic salts increases enough at a temperature ($T\Delta S > \Delta H$), the dispersion of inorganic salts into the pores of zeolites occurs spontaneously ($\Delta G < 0$).

MoO_3 on NaY. In contrast to NaZSM-5, the NaY zeolite has larger pores with 7.8 Å and β cage with diameter of 13 Å (14) and the MoO_3 dispersion amount in the NaY zeolite is slightly increased, arriving at 0.24 g/g, which corresponds to 0.034 g for each 100 m^2 of NaY internal surface. The value is still much less than that on the surface of the γ-Al_2O_3 support (only about 29%).

MoO_3 on MCM-41. Since a MCM-41 molecular sieve has a larger pore size with nearly 30 Å, the dispersion of MoO_3 into the pores of MCM-41 is slightly limited by the pore structure of the MCM-41 molecular sieve. At 0.45 or over 0.45 g/g of MoO_3/MCM-41 ratio, we still could not observe characteristic XRD peaks of crystalline MoO_3. However, if MoO_3 loading in MCM-41 molecular sieve is up to 0.50 g/g, the crystallinity (2θ at 1–4°) assigned to the MCM-41 molecular sieve partially decreases, which indicates changes in structure of the MCM-41 molecular sieve by dispersing MoO_3.

In summary, it is suggested that the dispersion capacity of MoO_3 on zeolite supports is mainly related to the internal surface area and pore size of the zeolites, and the zeolites with larger pores exhibit higher dispersion capacity.

$CuCl_2$ on supports. $CuCl_2$ on γ-Al_2O_3. The dispersion capacity of $CuCl_2 2H_2O$ on γ-Al_2O_3 is 0.20 g/g, corresponding to dispersion capacity of 0.077 g of $CuCl_2$ on 100 m^2 of γ-Al_2O_3 surface. By taking 1.80 Å as the radius of the Cl^- ion (20, 21) Xie *et al.* (15, 17) estimated the close-packed monolayer capacity at 0.10 g $CuCl_2$/100 m^2 of γ-Al_2O_3 surface, which suggests that $CuCl_2$ forms a submonolayer covering about 77% of the γ-Al_2O_3 surface.

$CuCl_2$ on NaZSM-5. The dispersion of $CuCl_2 2H_2O$ into NaZSM-5 zeolite is about 0.263 g of each 1 g of NaZSM-5, corresponding to the dispersion capacity of 0.058 g of $CuCl_2$ on 100 m^2 of NaZSM-5 internal surface. As compared with MoO_3/NaZSM-5, the dispersion capacity of $CuCl_2$ into NaZSM-5 zeolite is relatively high. The dispersion capacity of MoO_3 into NaZSM-5 zeolite is only 21% of MoO_3 on γ-Al_2O_3 surface, but the capacity of $CuCl_2$ into NaZSM-5 arrived at 75% of $CuCl_2$ on the γ-Al_2O_3 surface. The phenomenon may be interpreted by the differences in molecular structures for $CuCl_2$ and MoO_3. The dynamic diameter of $CuCl_2$ (3.6 Å) is much less than that of MoO_3 (5.0 Å).

Additionally, we found that the solid ion-exchange occurs at heating temperature while the inorganic salt contains cations. In the $CuCl_2$/NaZSM-5 sample, Na^+ cations in NaZSM-5 zeolite were exchanged for Cu^{2+} at 573–773 K, forming CuZSM-5 zeolite. The solid ion-exchange capacity is mainly related to the Na^+ content in NaZSM-5, and one Cu^{2+} is only exchanged with two Na^+. Because the Na^+ content in NaZSM-5 is very low (less than 2 wt% of NaZSM-5), the solid ion-exchange capacity is relatively limited, as compared with the dispersion method. For example, we observed that the solid ion-exchange capacity of NaZSM-5 with $CuCl_2$ is about 0.02 g/g, and the dispersion of $CuCl_2 2H_2O$ into NaZSM-5 is about 0.20 g/g. Notably, there are some obvious differences between the solid ion-exchange with the dispersion in the following: (1) The $CuCl_2$ into NaZSM-5 zeolite prepared by the dispersion could be washed away by water, and the Cu^{2+} in NaZSM-5 prepared by solid ion-exchange could not; (2) Both cations and anions are dispersed in the pores of zeolites prepared from dispersion method, and in contrast, only cations exist in the pores of zeolites prepared from the ion-exchange method;

(3) Metal oxides not having ion-exchange ability can be dispersed in zeolites by using the dispersion method, and these metal oxides cannot enter the pores of zeolites by solid ion-exchange procedures; (4) Considering the low capacity of solid ion-exchange, we thus ignore the contribution for solid ion-exchange reaction in the present study.

$CuCl_2$ on NaY. The dispersion of $CuCl_2 2H_2O$ into NaY zeolites is about 0.53 g for each 1 gram of NaZSM-5, corresponding to the dispersion capacity of 0.058 g of $CuCl_2$ on 100 m^2 of NaY internal surface, which is the same as that on NaZSM-5 channels. The results may indicate that the dispersion of $CuCl_2$ into zeolites is not mainly influenced by the structure of NaZSM-5 and NaY zeolites.

$NiCl_2 6H_2O$ on supports. $NiCl_2 6H_2O$ on γ-Al_2O_3. Both $NiCl_2$ and $NiCl_2 6H_2O$ easily disperse onto the surface of γ-Al_2O_3 at room temperature as a close-packed monolayer model, and the dispersion capacity of $NiCl_2$ is 0.093 g for 100 m^2 of Al_2O_3 surface.

$NiCl_2 6H_2O$ on NaZSM-5. In contrast to γ-Al_2O_3, the $NiCl_2 6H_2O$ could not disperse into NaZSM-5 channels at room temperature. As observed in Figs. 4b–4e, the XRD peaks assigned to $NiCl_2 6H_2O$ in mechanical mixtures is the same as those of the samples placed at room temperature for 36 h. The results may be explained by larger diameter of $NiCl_2 6H_2O$ (about 8–9 Å) relative to the pore openning of NaZSM-5 (5.6 Å) (14, 20, 21).

However, the dispersion of $NiCl_2 6H_2O$ into the channels of NaZSM-5 zeolites occurs when the sample is heating up to 433 K. As shown in Figs. 4f and 4g, the XRD peaks assigned to $NiCl_2 6H_2O$/NaZSM-5 in mechanical mixtures completely disappear after the mixtures are heated at 433 K for 24 h. The dispersion capacity of $NiCl_2 6H_2O$ is 0.045 g of 100 m^2 of NaZSM-5 internal surface. Increasing the temperature from room temperature to 433 K, leads to the dehydration of $NiCl_2 6H_2O$, giving $NiCl_2$ with dynamic diameter of 3.6 Å, much smaller than 5.6 Å (pore size of NaZSM-5). Of course, at high temperatures (443 K), $NiCl_2$ mobility is higher in NaZSM-5, thus leading to higher dispersion.

$NiCl_2 6H_2O$ on NaY. The same as the dispersion of $NiCl_2 6H_2O$ on γ-Al_2O_3, the $NiCl_2 6H_2O$ could disperse into the pores of NaY zeolites. Placement of the $NiCl_2 6H_2O$/NaY mixture at room temperature for 24 h results in the disappearance of characteristic XRD peaks of crystalline $NiCl_2 6H_2O$. Considering that the NaY zeolites has a β cage with diameter of 13 Å and the windows of 7.8 Å, the $NiCl_2 6H_2O$ molecule could easily disperse into the β cage of the NaY zeolite.

$Ni(NO_3)_2 6H_2O$ on NaZSM-5 and NaY. The same as the $NiCl_2 6H_2O$/NaZSM-5 sample, the $Ni(NO_3)_2 6H_2O$/NaZSM-5 system also shows the dispersion selectivity for zeolite pores. We observed that $Ni(NO_3)_2 6H_2O$ could not disperse into the channels of NaZSM-5 zeolite at room temperature, which is also attributed to the larger diameter of $Ni(NO_3)_2 6H_2O$ (9–10 Å) (21, 28) and the smaller channel of NaZSM-5 (29). However, the $Ni(NO_3)_2 6H_2O$ could disperse into the NaY zeolite at room temperature. The dispersion of $Ni(NO_3)_2 6H_2O$ into NaY zeolite may be related to the partial dehydration of $Ni(NO_3)_2 6H_2O$ at room temperature, forming $Ni(NO_3)_2(6-x)H_2O$ (x = number of water molecules lost) which has a size closed to 7.8 Å of NaY pore.

Thermal Analysis

As observed in Fig. 5, DTA curves of $CuCl_2 2H_2O$/NaZSM-5 sample ($CuCl_2 2H_2O$/NaZSM-5 at 0–0.22 g/g) treated at 723 K for 24 h, do not exhibit the peak assigned to melting point of $CuCl_2$. The results suggest that there is no $CuCl_2$ crystalline phase in the sample, relative to the facts: (i) the crystal cell of $CuCl_2$ is very small (<10 Å); (ii) internal surface area of the zeolite is very large as compared with the external surface area of the zeolite. For example, outside surface area of NaZSM-5 with particle size of 10 $\mu \times 2\ \mu \times 2\ \mu$, is less than 1% of total surface area; (iii) the pore size of NaZSM-5 is about 5.6 Å, we proposed that $CuCl_2$ highly disperses into channels of NaZSM-5 zeolite.

The Factors for Dispersion of Inorganic Salts into the Surface of Supports

As observed in Figs. 1–4, the experimental results are summarized:

(1) All of inorganic salts with various dynamic diameter easily disperse on the surface of γ-Al_2O_3 support. For example, MoO_3 disperses on γ-Al_2O_3 as a close-packed monolayer model; $CuCl_2$ disperses on γ-Al_2O_3 as a submonolayer model; $NiCl_2 6H_2O$ highly dispersed on γ-Al_2O_3. The dispersion capacity of inorganic salts is proportional to the surface area of supports.

(2) As compared with γ-Al_2O_3, the inorganic salts selectively disperse into the channels of NaZSM-5 zeolite due to the limitation of channel size. Inorganic salts having diameters smaller or similar to the channel size of NaZSM-5 zeolite could disperse into NaZSM-5 zeolite, while salts having the diameter larger than channel could not. For example, a molecule of MoO_3 with diameter of about 5.0 Å and molecules of $CuCl_2$ and $NiCl_2$ with diameters of 3.6 Å could disperse into NaZSM-5 zeolite, while molecules such as $NiCl_2 6H_2O$ and $Ni(NO_3)_2 6H_2O$ with diameter greater than 5.6 Å could not.

(3) The dispersion capacity of inorganic salts on the surface of supports is strongly influenced by the type of support which is interpreted to relate to the pore size of the supports. For MoO_3/supports, the dispersion capacity is mainly dependent on the pore size of the supports in addition to the surface area. The order of the dispersion capacity of MoO_3 on the supports is: γ-Al_2O_3 (0.12 g of 100 m^2 of the surface) $\gg$ MCM-41 (0.045) > NaY (0.034) > NaZSM-5

(0.025). Comparatively, the pore size effect of supports for $CuCl_2$ with smaller diameters was weaker, and the order for the dispersion capacity was as follows: γ-Al_2O_3 (0.077) > NaY (0.058) = NaZSM-5 (0.058).

It is suggested that three factors (the surface area of the zeolites, the pore sizes of zeolites, and the dynamic diameter of inorganic salts) play very important roles for the dispersion of inorganic salts into zeolites. It is reasonable that the dispersion of inorganic salts into zeolites only occurs under the condition that the diameter of inorganic salts is smaller or similar to the pore size of zeolites. Such a conclusion has been not found in the systems of inorganic salts on γ-Al_2O_3 because the pore sizes of γ-Al_2O_3 is much larger than that of all of inorganic salts.

Investigation of Pore Sizes for Dispersion of Inorganic Salts into Zeolites

MoO_3 on NaZSM-5. As shown in Fig. 6, the MoO_3-NaZSM-5 sample (MoO_3/NaZSM-5 ratio of 0.088 g/g, treatment by heating at 723 K for 24 h) exhibits Langmuir-type adsorption of the water (diameter of 3.0 Å) (14, 28), but it does not adsorb on normal hexane (diameter of 4.3 Å) (18, 28). The results indicate that the pore size of the MoO_3/NaZSM-5 sample is in the range of 3.0–4.3 Å, which is explained that the dispersion of MoO_3 into the channels of NaZSM-5 zeolite, reducing the channel size of NaZSM-5 zeolite.

MoO_3 on NaY. As observed in Figs. 7–10, the isotherms for various probing molecules on a series of MoO_3/NaY samples with various MoO_3 loadings exhibit quite different adsorption properties (14, 28, 31). The sample with MoO_3/NaY ratio at 0.08 g/g shows Langmuir-type adsorption for cumene (6.8 Å), indicating the pore size at 6.8–8.0 Å. Increasing the MoO_3 loading in NaY zeolite to 0.16 g/g, the sample shows Langmuir-type adsorption for cyclohexane, but it could not adsorb cumene, suggesting the pore size is in the range of 6–6.8 Å. With an increase of MoO_3 loading in NaY zeolite to 0.21 g/g, the sample exhibits Langmuir-type isotherms for normal-hexane, but not for cyclohexane, demonstrating the pore size in 4.4–6.0 Å. With further increase of MoO_3 loading in the NaY zeolite to 0.24 g/g, the sample only adsorbs water, indicating the pore size in 3.0–4.3 Å. From these facts, it is obvious that the pore size of the MoO_3–NaY mixtures is easily controlled by the loadings of MoO_3 in NaY zeolite.

Considering the results of MoO_3/NaY samples, it is reasonable that MoO_3 with loadings at 0–0.08 g/g selectivity disperses inside of β cage (13 Å) of NaY, because we observed that the pore size of NaY is almost not influenced by 0–0.08 g/g MoO_3 loadings. In contrast, MoO_3 with loadings at 0.16–0.24 g/g mainly disperse into near pore windows of NaY zeolite, because the pore size of NaY is remarkably influenced by the 0.16–0.24 g/g MoO_3 loadings, as shown in Fig. 13.

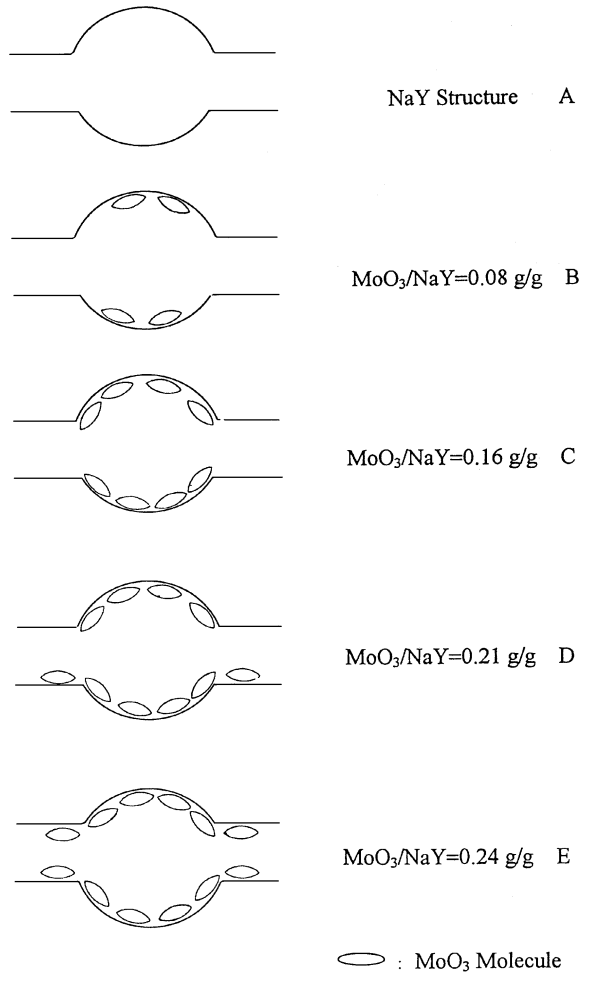

FIG. 13. The proposed dispersion of MoO_3 into NaY zeolite with various MoO_3 loadings: (a) NaY structure; (b) MoO_3/NaY = 0.08 g/g, the sample adsorbed cumene; (c) MoO_3/NaY = 0.16 g/g, the sample adsorbed cyclohexane, and did not adsorb cumene; (d) MoO_3/NaY = 0.21 g/g; the sample adsorbed normal hexane and did not adsorb cyclohexane; (e) MoO_3/NaY = 0.24 g/g; the sample only adsorbed water and did not adsorb normal hexane. (⬭: MoO_3 molecule).

MoO_3 on MCM-41. As observed in Fig. 11, the pore size of MCM-41 is significantly larger than and MoO_3/MCM-41 (25 Å). This demonstrates that the pore size of the MCM-41 molecular sieve could be modified by the dispersion of inorganic salts.

The Control of Pore Size of Zeolites

From above results, we observed that the pore sizes of salt/zeolite systems are easily influenced by the loading of inorganic salts. For example, the MoO_3–NaY system exhibits the pore sizes at 6.8–8.0, 6.0–6.8, 4.3–6.0, and 3.0–4.3 Å with MoO_3 loadings at 0.08, 0.16, 0.21, and 0.24 g/g, respectively. These results have demonstrated that the salts dispersed inside of zeolite pores. Therefore, it is suggested that we could design the pore size of zeolites to various degrees by dispersing various loadings of inorganic salts

into zeolites, which is very important for the application on catalysis by zeolites because the reactants required suitable pores of zeolites.

Recently, Wang *et al.* (12, 13) reported that MoO_3/HZSM-5 catalyst is very active for catalytic conversion of methane to benzene at 773–923 K. The catalyst with MoO_3/HZSM-5 ratio of 0.02–0.03 g/g give the highest catalytic activity and selectivity, and when the MoO_3 loading in HZSM-5 zeolite is increased to 0.10 g/g, the catalyst lose its activity completely. This is a good example for assembly of active component (MoO_3) into zeolite with product selectivity (HZSM-5) and for design of suitable pore size to catalytic reactions. Isotherm measurements (31) show that MoO_3/HZSM-5 at 0.02 g/g give the largest value for the adsorption of methane and benzene; When the MoO_3 loading in HZSM-5 zeolite was increased to 0.088 g/g, the sample do not adsorb the methane. Because catalysis is a surface phenomenon, it is reasonable that the MoO_3/HZSM-5 sample with the largest value for methane adsorption could exhibit the highest catalytic activity for methane conversion, and that the catalyst without methane adsorption is completely inactive for the methane conversion.

In general, the choice of various pore size in zeolites is usually by using various types of zeolites (14, 31–33) (a zeolite with pore size of 3–4 Å, NaZSM-5 zeolite with pore size of 6 Å, and NaY zeolite with pore size of 8 Å, respectively). In this study, we develop a new method to prepare the samples with various pore sizes such as NaY varying from 3 to 8 Å, by using the dispersion of inorganic salts into the pores of zeolites.

Electron Probe Microanalyzer

As a typical run, we investigate the distribution of Mo species in NaZSM-5 crystal, and the EPMA results of four points on the crystal paralleled *c* axis, exhibit the similar value for Mo species (MoO_3/NaZSM-5 = 0.05 g/g), which is good agreement with the MoO_3 loading in the channels of NaZSM-5. Furthermore, EPMA results of three points were determined in the NaZSM-5 crystal paralleled *a* axis, giving the same value for the ratio of MoO_3/NaZSM-5 (0.05 g/g). The fact confirms that the Mo atoms almost homogeneously distribute inside of NaZSM-5 channels.

To understand the structural state of inorganic salts on the supports, Jin *et al.* (34) study NiO/γ-Al_2O_3 system (NiO/γ-Al_2O_3 ratio of 0.10 and 0.20 g/g, monolayer dispersion capacity is 0.24 g/g NiO/γ-Al_2O_3) by EXAFS technique. EXAFS spectroscopy shows that the Ni–Ni coordination numbers characterizing the NiO/γ-Al_2O_3 with NiO loadings at 0.10 and 0.20 g/g are 2.0 and 3.5, respectively, which are obviously distinguishable from 12, the value of NiO crystalline. Considering the theoretical value of Ni–Ni coordination numbers at 4.0, the EXAFS results of NiO/γ-Al_2O_3 samples provide evidence that NiO in the samples disperses as *monolayer* onto the surface of γ-Al_2O_3. Recently, we have prepared NiO/NaY sample (NiO/NaY ratio of 0.15 g/g) by the dispersion of $Ni(NO_3)_2 6H_2O$ into NaY zeolite, and followed by heating at 723 K for 2 h to remove NO_2 and H_2O. EXAFS spectroscopy of the NiO/NaY sample shows the Ni–Ni coordination numbers at near 2.5, demonstrating that NiO distributes randomly and do not form clusters or patches in the pores of zeolites.

Selective Catalytic Reduction of NO by Propylene

Correlation of catalytic data with infrared spectra, shows that the samples with a strong acidic OH groups appearing at 3610 cm^{-1} band exhibited relatively high catalytic conversion (samples 4 and 5) as compared with that of the samples without 3610 cm^{-1} band (samples 1, 3, and 6). In addition, $CuCl_2$/HZSM-5 with higher copper loading (sample 5) gave higher catalytic conversion (36–39%) than that of CuZSM-5 (sample 4) (18–21%). These results suggested that both highly dispersed copper species and protons in ZSM-5 zeolite would be very important for selective catalytic reduction of NO by propylene, which might be related to the synergetic effect of acidic sites and copper species in these catalysts.

The catalytic active sites by which hydrocarbons reduce NO over CuZSM-5 prepared from the ion-exchange method has largely been investigated by reaction kinetics and IR spectroscopy (35–37). They suggested that the catalytic active sites were from copper species, and there was no discussion on the effect of acidic sites in CuZSM-5.

It has been reported that the turnover frequency of NO conversion on CuZSM-5 prepared from the ion-exchange method had a linear relationship with the Si/Al ratio when the ion-exchange level was 90% or more (38), which indicated that the NO conversion is proportional to Cu loading in the CuZSM-5 catalyst.

In the present study, we suggested that propylene and NO are activated by acidic sites and copper species, respectively. More copper species would give higher catalytic activity. Because the $CuCl_2$/HZSM-5 catalyst prepared from the dispersion method is almost twice copper loading as the CuZSM-5 prepared from the ion-exchange procedure, it may be reasonable that the $CuCl_2$/HZSM-5 with a larger copper loading gives higher catalytic activity as the CuZSM-5.

Furthermore, we try to design and prepare catalysts of $CuCl_2$/MCM-41 (silicalite) and $CuCl_2$/MCM-41 (aluminosilicate) (39, 40). Catalytic data in the selective reduction of NO by propylene in the range of 300–600°C show that the activity for $CuCl_2$/MCM-41 (aluminosilicate) with a strong ν_{OH} at 3610 cm^{-1} is much higher than that for $CuCl_2$/MCM-41 (silicalite) without the 3610 cm^{-1} bands (40, 41), and details will be reported in the future.

CONCLUSION

The important conclusions of this study may be summarized as follows:

(1) The dispersion of inorganic salts in the pores of zeolites is strongly influenced by the pore size of the zeolites and the dynamic diameter of the inorganic salts, and it only occurred when the diameter of the inorganic salts was smaller or similar to the pore size of the zeolites.

(2) The dispersion capacity of inorganic salts on the surface of supports is related to the pore size of the zeolites. For MoO_3/supports, the dispersion capacity increased with increased the pore size, and the order of the dispersion capacity is: γ-$Al_2O_3 \gg$ MCM-41 > NaY > NaZSM-5. Comparatively, the pore size effect for dispersion of inorganic salts with linear molecules such as $CuCl_2$ is relatively weak, and the order for dispersion capacity is: γ-Al_2O_3 > NaY = NaZSM-5.

(3) The dispersion of inorganic salts into zeolites leads to a significant change in the pore size of samples. The MoO_3/NaZSM-5 sample with MoO_3 loading of 0.088 g/g showed the pore size of the sample ranged of 3.0–4.3 Å. A series of MoO_3/NaY samples exhibited the pore sizes at 6.8–8.0, 6.0–6.8, 4.3–6.0, and 3.0–4.3 Å with MoO_3 loadings at 0.08, 0.16, 0.21, and 0.24 g/g, respectively. It is suggested that we could design the pore size of zeolites to be various degrees by the dispersion of inorganic salts.

(4) The catalytic activity in the selective reduction of NO by propylene shows that a $CuCl_2$/HZSM-5 catalyst exhibits higher conversion at 300°C than that of CuZSM-5 prepared from the ion-exchange method. Correlation of catalytic data with infrared spectra for $CuCl_2$/HZSM-5, $CuCl_2$/NaZSM-5, and CuZSM-5 samples suggested that the catalytic sites would be assigned to the synergetic effect of protons and copper species.

ACKNOWLEDGMENTS

This work was supported by the Foundation of the State Education Commission of China, the National Natural Science Foundation of China, the National Advanced Materials Committee of China (NAMCC), the Foundation of Pan-Deng Plan in China, and the Foundation of Key Laboratory for Inorganic Synthesis and Preparative Chemistry.

REFERENCES

1. Delmon, B., Jacobs, P. A., and Poncelet, G., "Preparation of Catalyst." Elsevier Science, Amsterdam, 1976.
2. Poncelet, G., Grange, P., and Jacobs, P. A., "Preparation of Catalyst III." Elsevier Science, Amsterdam, 1983.
3. Yao, H. C., Yu, Y. F., and Otto, K., *J. Catal.* **56**, 21 (1979).
4. Lee, G. Y., and Zhao, J. C., *Petrochem. Technol. (China)* **16**, 266 (1987).
5. Iwamoto, M., Yokoo, S., Sakai, K., and Kagawa, S., *J. Chem. Soc., Faraday Trans. I* **77**, 1629 (1981).
6. Iwamoto, M., Yahiro, H., Tanada, K., Mizuno, N., Mine, Y., and Kagawa, S., *J. Phys. Chem.* **95**, 3727 (1991).
7. Li, Y., and Hall, W. K., *J. Catal.* **129**, 202 (1991).
8. Li, Y., and Armor, J. N., *Appl. Catal.* **76**, 21 (1991).
9. Shelef, M., *Catal. Lett.* **15**, 305 (1992).
10. Rao, L.-F., Fukuoka, A., Kosugi, N., Kuroda, H., and Ichikawa, M., *J. Phys. Chem.* **94**, 5317 (1990).
11. Xu, Z., Xiao, F. S., Purnell, S. K., Alexeev, O., Kawi, S., Deutsch, S. E., and Gates, B. C., *Nature* **372**, 346 (1994).
12. Wang, L.-S., Tao, L.-X., Xie, M.-S., Xu, G.-F., Huang, J.-S., and Xu, Y.-D., *Catal. Lett.* **21**, 35 (1993).
13. Xie, M.-S., Wang, L.-S., Tao, L.-X., Xu, G.-F., Wang, X.-L., Xu, Y., Huang, J., and Guo, X.-X., "7th Japan-China-USA Symposium on Catalysis, July 1995, Tokyo, Japan."
14. Breck, D. W., "Zeolite Molecular Sieves." Wiley, New York, 1974.
15. Xie, Y.-C., and Tang, Y.-Q., *Adv. Catal.* **37**, 1 (1990).
16. Lipsch, J. M. J. G., and Schuit, G. C. A., *J. Catal.* **15**, 174 (1969).
17. Xie, Y. C., Gui, L. L., Liu, Y. J., Zhang, Y. F., Zhao, B. Y., Yang, N. F., Guo, Q. L., Duan, L. Y., Huang, H. Z., Cai, X. H., and Tang, Y. Q., *Proc. 8th Int. Congr. Catal.* **5**, 147 (1984).
18. Barrer, R. M., "Hydrothermal Chemistry of Zeolites." Academic Press, London, 1982.
19. Kresge, C. T., Leonowicz, M. E., Roth, W. J., Vartuli, J. C., and Beck, J. S., *Nature* **359**, 710 (1992).
20. Wells, A. F. "Structural Inorganic Chemistry," 4th ed., Oxford Univ. Press, London/New York, 1975.
21. Shriver, D. F., Atkins, P. W., and Langford, C. H., "Inorganic Chemistry," Freeman, New York, 1990.
22. Xie, Y. C., Zhang, H. X., and Wang, R. H., *Sci. Sin. (Chinese)*, 337 (1980). [Sci. Sin. (English) **23**, 980 (1980)]
23. Xiao, F.-S., Xu, W., Qiu, S., and Xu, R., *J. Mater. Chem.* **4**, 735 (1994).
24. Xiao, F.-S., Xu, W., Qiu, S., and Xu, R., *J. Catal. Lett.* **26**, 209 (1994).
25. Liu, Y. J., Xie, Y. C., Ming, J., Liu, J., and Tang, Y. Q., *J. Catal. (Chinese)* **3**, 262 (1982).
26. Argauer, R. J., and Landolt, G. R., U.S. Patent, 3,702,866 (1972).
27. Fransen, T., Van Berge, P. C., and Mars, P., *in* "Preparation of Catalysts" (B. Delmon, P. A. Jacobs, and G. Poncelet, Eds.), p. 405. Elsevier, Amsterdam, 1976.
28. Rabo, J. A., "Zeolite Chemistry and Catalysis," ACS Monograph 171. Am. Chem. Soc., Washington, DC, 1976.
29. Jacobs, P. A., and von Ballmoos, R., *J. Phys. Chem.* **86**, 3050 (1982).
30. Chu, C. T.-W., and Chang, C. D., *J. Phys. Chem.* **89**, 1569 (1985).
31. Murakami, Y., Iijima, A., and Ward, J. W., "New Developments in Zeolite Science and Technology." Kodansha, Tokyo, 1986.
32. Xie, Y. C., Xu, X. P., Wu, G. B., and Tang, Y. Q., "Proc. Chin. Congr. Catal., 4th, Tianjin, 1-E-29, 1988."
33. Xiao, F.-S., and Xu, R., 7th National Catalysis Meeting of China, Oct. 12–18, 1996, Xiamen, P. R. China.
34. Jin, X. L., Cai, X. H., Ge, Z. H., Xie, Y. C., and Tang, Y. Q., *Acta Phys.-Chem. Sin. (China)* **5**, 206 (1989).
35. Burch, R., Millington, P. J., and Walker, A. P., *Appl. Catal. B* **3**, 295 (1994).
36. Simits, R., and Iwasawa, Y., *Appl. Catal. B* **6**, L201 (1995).
37. Hayes, N. W., Joyer, R. W., and Shpiro, E. S., *Appl. Catal. B* **8**, 343 (1996).
38. Moretti, G., *Catal. Lett.* **28**, 143 (1994).
39. Kresge, C. T., Leonowicz, M. E., Roth, W. J., Vartuli, J. C., and Beck, J. S., *Nature* **359**, 710 (1992).
40. Jia, M. J., Lin, W. Y., Zhang, W. X., Xiao, F.-S., Pang, W. Q., and Wu, T. H., unpublished results.
41. Corma, A., Fornes, V., Navarro, M. T., and Perez-Pariente, J., *J. Catal.* **148**, 569 (1994).